Research Article

Journal of Environmental Nanotechnology

Multi-objective Optimization of Bamboo-madar Fiber Reinforced Composites for Lightweight Automotive Applications using Machine Learning and Genetic Algorithms

Raj Kumar Gupta[1], S. Mayakannan[2*], Sivakumar Vijayaraghavalu[3,4], M. M. Poornima[5], S. Nanthakumar[6] and N. A. Bhaskaran[7]

[1]Department of Physics, Sardar Vallabhbhai Patel College, Bhabua, BR, India
[2]Department of Mechanical Engineering, Rathinam Technical Campus, Coimbatore, TN, India
[3]Department of Life Sciences (Zoology), Manipur University, Imphal, MN, India
[4]Department of Medical Sciences and Technology, IIT Madras, TN, India
[5]Department of Computer Science and Engineering, Koneru Lakshmaiah Education Foundation, Vaddeswaram, Guntur, AP, India
[6]Department of Mechanical Engineering, PSG Institute of Technology and Applied Research, Neelambur, Coimbatore, TN, India
[7]Department of Artificial Intelligence and Data Science, Arjun College of Technology, Coimbatore, TN, India
Received: 01.10.2024 Accepted: 23.12.2024 Published: 30.12.2024
*kannanarchieves@gmail.com

ABSTRACT

The accelerated growth of the automobile industry intensifies sustainability issues, primarily because of its significant carbon emission and the resulting impacts on global environmental systems. These emissions are directly correlated with fuel usage, which is subsequently affected by the material weight utilized in automobile systems. This research utilized machine learning (ML) techniques to optimize the production parameters of natural fiber (NF)-reinforced materials for airplane body applications. A study was conducted using the Taguchi optimization approach to investigate the effect of different fiber lengths, concentrations of sodium hydroxide treatment, Nano SiO_2 and hybrid fiber (bamboo fibers, and madar fibers (BMF)) on the performance of the material. In order to find the best combination of the factors that were considered for automobile structural applications with low fuel consumption (low carbon emissions) and high reliability, multi-objective optimization (MOO) methods like additive ratio assessment (ARAS) and genetic algorithms (GA) were utilized within the MATLAB programming environment. With R^2 values above 80%, the regression analysis-derived models demonstrated good predictive accuracy. The optimization of ARAS for the developed composite by the GA identified the optimal process parameters for achieving lightweight materials suitable for automobile applications as 35% BMF, 10% Nano SiO_2 at a fiber length of 24mm, and a 9 % concentration of sodium hydroxide, with ARAS reaching its maximum level of unity.

Keywords: ANOVA; Machine learning; Single objective optimization; ARAS; Regression analysis.

1. INTRODUCTION

Researchers have opted to investigate natural fibers rather than synthetic fibers due to the necessity for cost-effective and environmentally sustainable materials. This research focuses on the mechanical properties of epoxy composites reinforced with bamboo and bagasse fibers (Natrayan *et al.* 2024). Plant-based composites are regarded as future materials that provide sustainability, environmental friendliness, and green chemistry, employed across various industries (Yusoff *et al.* 2023). Environmentally friendly polymer composites composed of plant-based natural fibers, such as bamboo fiber, roselle fiber, aloe vera fiber, and kenaf fiber, are essential for contemporary sustainability efforts. They provide a reduced carbon footprint, enhanced biodegradability, superior specific strength, and improved thermal and acoustic properties (Vijayan *et al.* 2023).

The influence of fiber ply orientation on the flexural and impact characteristics of sisal, bamboo, and hybrid fiber-reinforced composites subjected to alkaline treatment and composites were produced by the Taguchi L9 Orthogonal array and hand layup method. Findings indicate that 90° orientations give optimal mechanical strength with bamboo and hybrid fibers exhibiting the highest flexural (281.25 MPa) and impact (46 kJ/m²) strengths (Ganta and Patel, 2024). The advantages of hybrid composites emphasize their mechanical performance and environmental benefits. The study notes a 22% increase in flexural strength and a 21.6% rise in modulus with 30% bamboo fiber. Glass fiber stacking shows improved tensile strength and elasticity as fiber weight increases, indicating that combining natural and synthetic fibers leads to superior performance in various applications (Premnath *et al.* 2024).

Five laminates with varying Madar fiber/ bran filler ratios were tested, showing that increasing Madar fiber content improved mechanical properties such as tensile strength (20.85 MPa), flexural strength (24.14 MPa), and impact energy (23 J) (Raja *et al.* 2023). The composite made of glass/Madar fibers and porcelain particles with epoxy reinforcement showed successful integration of porcelain fillers, with improved viscoelastic properties (4.2%) and thermal stability up to 357 °C, making it suitable for structural applications (Raja *et al.* 2024b). Various stacking sequences were tested using a hand-layup method, revealing that jute fibers contributed more strength while Madar fibers provided strain and toughness. The tensile strength of hybrid (Madar and bamboo) fiber composites was validated with an FEA model in ANSYS, generating a regression equation for tensile properties based on ply angles. This work highlights the potential of natural fibers as alternatives to synthetic fibers in high-end applications (Elango *et al.* 2022).

The mechanical properties of bamboo and pineapple leaf fiber-reinforced PLA composites with input parameters included chemical treatments (NaOH, KOH, Na_2CO_3), concentration (1–3%), and treatment time (2–6 hours) were analyzed. Optimal conditions were achieved with (2%) NaOH for 4 hours for bamboo fibers and Na_2CO_3 (1%) for 6 hours for pineapple fibers (Gorrepotu *et al.* 2023). This study examined the mechanical properties of bamboo fiber bundles extracted from different radial parts of the stem after heat treatment. The findings offer a basis for optimizing bamboo materials for industrial applications under heat treatment (Cui *et al.* 2023). The study focused on developing bamboo fiber-reinforced composites with four different epoxy matrices and 30% fiber loading. A VIKOR-based material selection process recommended S_2 composites for automotive interiors, though issues like hydrophilicity and interfacial bonding remained challenges (Saha *et al.* 2023).

Mechanical testing revealed that while bamboo reinforcement did not alter the physical properties of the matrix, bamboo fibers exhibited superior tensile modulus (9.6 GPa) compared to bamboo strips (7.7 GPa). SEM analysis confirmed good material interaction between the reinforcements and matrix (Richmond *et al.* 2022). This study optimized the reinforcement of epoxy composites with bamboo and glass fibers for automotive applications using the Taguchi L9 orthogonal array. Results showed high tensile (232.1 MPa) and flexural strength (536.33 MPa) after alkali treatment and optimization of fiber content (Tadesse *et al.* 2023). SEM analysis revealed improved fiber-matrix bonding. The study promotes sustainable material development using natural resources and repurposed waste (Anand and Ekbote, 2024). The model showed high accuracy and outperforming traditional methods. Bamboo fiber percentage was identified as a key predictor for tensile strength, demonstrating its potential in improving the performance (Bajaro and Silva, 2023). The higher bamboo fiber content increased water absorption and decreased density due to porosity (Abessolo *et al.* 2022). Bamboo fiber composites with moderate fiber length and separation demonstrated the best mechanical properties, including a flexural strength of 97.90 MPa and a storage modulus of 5198 MPa. Proper fiber separation and size were key factors in enhancing interfacial bonding and mechanical performance. Bamboo fibers significantly improved the mechanical strength, thermal conductivity, and density of autoclaved aerated concrete compared to basalt fibers. (Quan *et al.* 2023).

This study focused on ice composites reinforced with various fiber materials, including bamboo fibers and waste mask material. Different fiber types, content, and orientations were tested for their effects on mechanical properties like stiffness, elastic modulus, and tensile strength. The study creatively used laser pointers and mirrors to magnify small deformations in ice composites, providing innovative methods to measure material behavior under room temperature conditions (Zhao *et al.* 2021). This research explored madar fiber-reinforced epoxy composites with porcelain filler for biomedical instrumentation. XRD and FTIR analyses confirmed the improvement in crystallinity and bonding. The composite showed excellent mechanical properties, with tensile strength of 51.28 MPa, flexural strength of 54.21 MPa, and impact strength of 0.0155 kJ/m² (Raja *et al.* 2024a). The composites, prepared using conventional compression molding, demonstrated enhanced mechanical properties with 28 wt.% madar fiber and 7 wt.% SBA fillers, showing a tensile strength of 61 MPa, flexural strength of 147 MPa, and impact strength of 54 kJ/m² (Chandrika *et al.* 2022). The research focused on the mechanical properties of madar and gongura fiber reinforced polyester composites. These lightweight fibers, combined with polyester resin, were found to be effective for various industrial applications (Yoganandam *et al.* 2020). Alkali treated gongura and Hibiscus cannabinus fiber showed the results of r tensile (34.720 N/mm²), flexural (77.957 MPa), and flexural modulus (1548.588 GPa) (Marichelvam *et al.* 2023).

This study investigates polyvinyl ester (VE) composites reinforced with discarded and (ESP). Using a multi-criteria decision-making (MCDM) approach with CRITIC-TODIM, optimal mechanical properties were achieved with 60 wt% cigarette filter fiber (CFF), 20 mm fiber length, and 3 wt% chicken eggshell powder filler (Vijayananth *et al.* 2024). Mechanical properties were optimized using the CRITIC-WASPAS MCDM approach, with 5 wt% eggshell powder and 30 wt% Borassus fruit fiber - cigarette butts fiber yielding tensile strength of 52.26 MPa, flexural strength of 37.76 MPa, and impact strength of 36.87 J/m (Kavimani *et al.* 2024). Orthogonal tests and AHP-CRITIC analysis revealed that 35% expanded polystyrene (EPS), 0.9%

polyoxymethylene (POM) and a water-binder ratio of 0.21 provided optimal mechanical and insulation properties. Compared to other natural fibers, Bamboo-Madar fibers are ideal for lightweight automotive composites due to their high specific strength, modulus, and toughness, ensuring durability and reduced density. Alkaline treatment enhances fiber-matrix bonding, improving tensile, flexural, and impact properties. Their sustainability and optimized parameters support eco-friendly and efficient automotive designs. Unlike synthetic fibers, they are biodegradable and environmentally friendly, reducing the carbon footprint.

The findings indicated that the utilization of symmetric cross-ply laminates enhances the performance of aircraft wing design. Authors developed methodologies for optimizing aircraft fuselage designs to enhance performance regarding compliance, weight, and natural frequency in first mode. To accomplish this, various heuristic multi-objective optimization approaches were employed, and their distinct outcomes were compared. The outcome of the study indicated an improvement in the structural effectiveness of the airplane fuselage according to the design specifications. This work is the first attempt to reduce carbon emissions by applying a GA on NFs hybridized with synthetic fibers to optimize materials for the manufacturing of low-fuel aircraft.

The current research investigates the feasibility of creating airplane body materials from NFs to reduce weight and, consequently, carbon emissions while maintaining performance standards. It aims to determine the appropriate proportion for substituting synthetic fibers with NFs (Madar and Bamboo) in the construction of airplane structures. Various optimization methods are employed; notably, the ML approach (GA) is utilized on models derived from multi-objective optimization (ARAS) and single-objective optimization (Taguchi) to obtain optimal blends of material manufacturing process parameters. The use of multi-objective optimization (MOO) methods like ARAS and genetic algorithms (GA) in this research enables the simultaneous optimization of conflicting objectives, which is critical for lightweight automotive composites. These methods provide enhanced accuracy, robustness, and adaptability, handling complex, nonlinear relationships between variables and ensuring reliable results even under varying experimental conditions. The primary goal of this endeavor is to enhance lightweight materials with the goal of decreasing automobile fuel consumption.

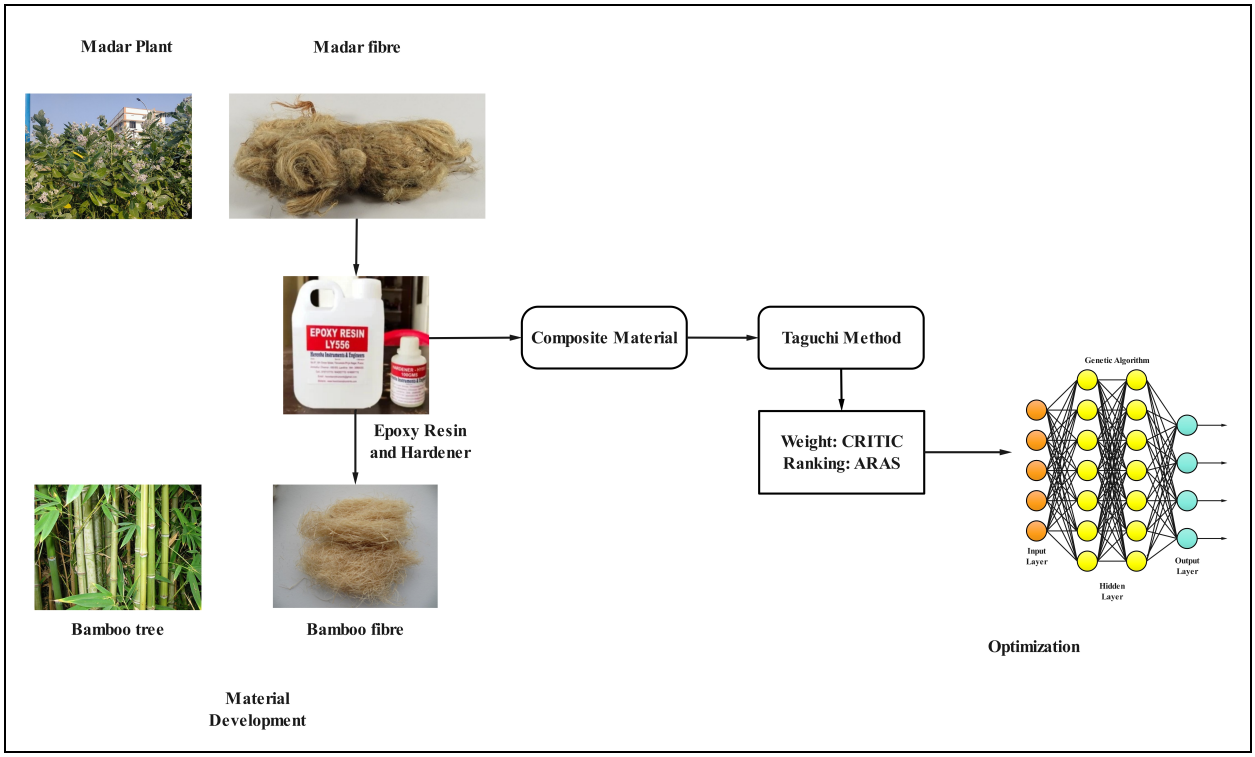

Fig. 1: Schematic view of research methodology

2. EXPERIMENTAL TECHNIQUES

Fig. 1 provides a schematic view of the research methodology. It outlines the procedures for developing new materials and the methods applied to optimization.

2.1 Fiber Treatment

The MF was procured from locally available madar leaves utilizing the process. Prior to alkalization, the isolated fibers were meticulously cleaned with

purified water and subsequently dried at 50°C for a full day. The desiccated MFs were subsequently subjected to treatment by immersion in an aqueous NaOH solution at varying concentrations, as outlined in the experimental design. The fibers that are submerged are kept in the solution at 70 °C for three hours. The fibers are subsequently subjected to a 5% acetic acid solution for de-alkalinization. Subsequent to de-alkalization, the fibers are meticulously cleansed in distilled water and dehydrated in an oven at 70 °C for 12 hours.

2.2 Composite Development

The hand layup technique was used to create the composites. The treated MF and BF were cut to the specified lengths according to the OA. Kovai Cheenu Enterprises, Coimbatore, Tamilnadu, India, provided the epoxy and hardener. The ratio of the epoxy to the matrix was 10:1, and chopped MF and BF were incorporated into the mixture as per the experimental layout and thoroughly mixed before being transferred into the exposed steel mold, measuring 300x300x3 mm. Initially, wax was applied to the mold to make the removal easier.

The composite was purged of trapped air using roller brushes, and the mixture was uniformly distributed throughout the mold cavity using brushes. After being placed in the hydraulic press, the mixes in the mold were kept there for 72 hours at a pressure of 15 MPa. This additionally facilitated the elimination of cavities inside the material. The molded materials were subsequently extracted and trimmed. Fig. 2 shows the production process of the composite. Distinct samples for various testing were extracted from the fabricated composites.

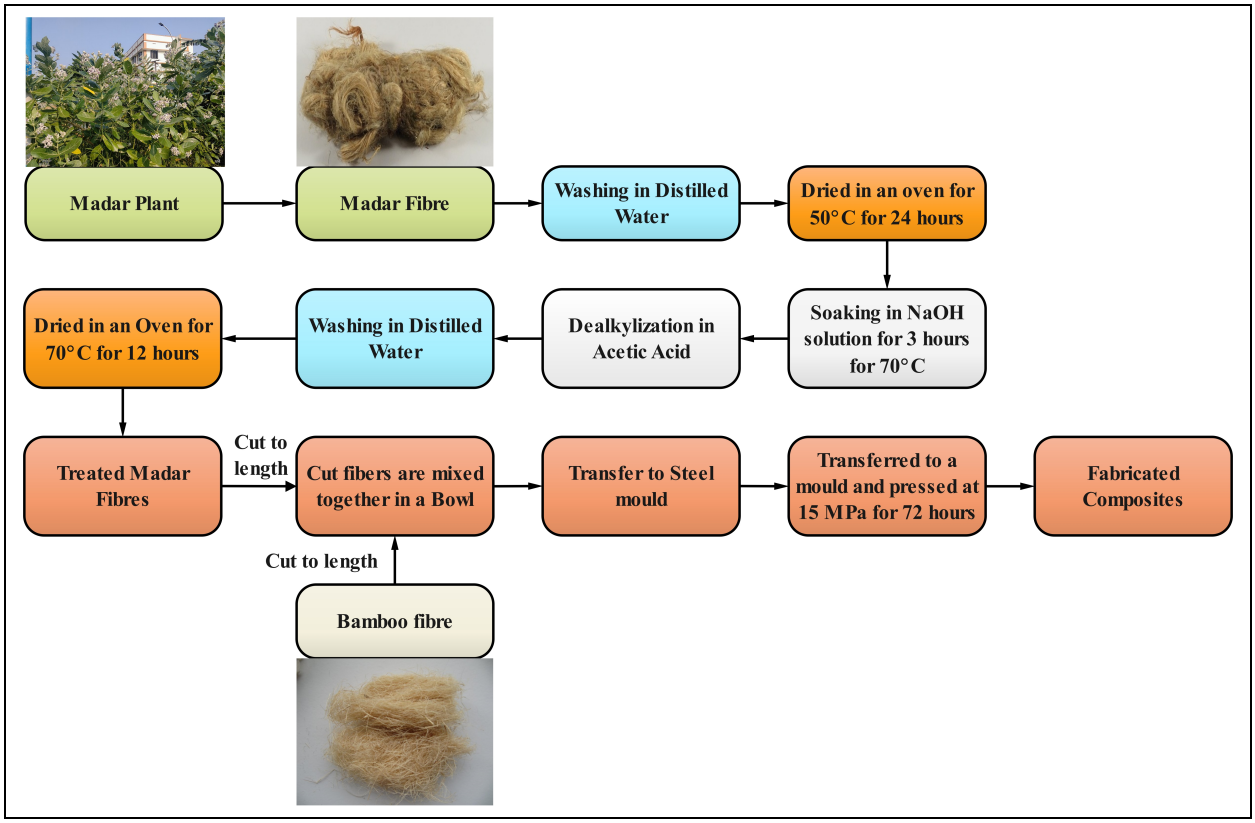

Fig. 2: Fabrication of composites

2.3 Physical and Mechanical Examinations

2.3.1 Physical Properties

The density of the materials was determined using the water displacement method, based on Archimedes' principle. The amount of water displaced was utilized to determine the material's density as per Eq. (1),

$$\rho = \frac{m}{v} \quad \ldots (1)$$

where, v signifies the volume of displaced water and ρ represents density, m denotes mass (measured directly using a digital weighing balance).

2.3.2 Mechanical Properties

ASTM D638-14 was followed to test the Tensile Strength (TS) of the manufactured composites. The procedure was carried out at a crosshead speed of 2 mm/min utilizing the UTM (Instron 5567). The TS was subsequently derived utilizing Eq (4).

$$\text{Stress} = \frac{\text{Force}}{\text{Area}} \quad \ldots (2)$$

$$\text{Tensile Strength} = \frac{\text{Load at Break}}{\text{(Actual width) x (Actual thickness)}} \quad \ldots (3)$$

The Instron 3365 UTM, configured with a length of span 40mm and a speed of crosshead 10mm/min, was employed to evaluate Flexural Strength (FS) of the composite in accordance with ASTM 7264-21. Dimensions of the flexural test specimen are 60×10×3mm.

FS was conducted on 3 specimens for every combination (run), and the mean was documented. The FS was subsequently calculated using Eq (2).

$$\text{FS} = \frac{3PL}{2bt^2} \quad \ldots (4)$$

Let L represent the sample length, P denote max applied stress, b signify width, and t indicate the thickness of specimens.

Using an instrumented pendulum from PANTECH (Model XC-50) set up at 1 × 220V × 60Hz, the impact test (Impact Strength (IS)) was performed. The test samples were prepared in accordance with the dimensions stated in ASTM D6110-18.

3. OPTIMIZATION

3.1 The Robust Parameter Design Methodology of Taguchi and ARAS

3.1.1 Taguchi Robust Experiment Design

Taguchi method of optimization identifies the ideal combination of multiple parameters to achieve the most favourable outcome. It is commenced by employing reduced variability through the S/N ratio technique, in which noise (unregulated consequences) is significantly diminished to enhance the anticipated (regulated) effect. This involves evaluating the measurable effect for highest recorded value (max), known as "higher the better," lowest recorded value (min), termed "lower the better". Accordingly, it is expected that variables like passenger satisfaction, safety, airport service quality, and consumer patronage will reach optimal levels hence the expression "the higher the better." The metrics of weight, maintenance costs, fuel consumption, maintenance duration, and flight delays are anticipated to reach their minimal values, so they are categorized as “lower the better.” The signal-to-noise ratios for optimal performance, minimal performance, and nominal performance are derived from Equations (5-7), accordingly.

$$\left(\frac{S}{N}\right)_{HTB} = -10 * \log_{10}\left(\frac{1}{n}\sum_{i=1}^{n}\frac{1}{y_i^2}\right) \quad \ldots (5)$$

$$\left(\frac{S}{N}\right)_{STB} = -10 * \log_{10}\left(\frac{1}{n}\sum_{i=1}^{n} y_i^2\right) \quad \ldots (6)$$

$$\left(\frac{S}{N}\right)_{NTB} = 10 * \log_{10}\left(\frac{1}{n}\sum_{i=1}^{n}\frac{\bar{y}^2}{s^2}\right) \quad \ldots (7)$$

In the orthogonal array, yi denotes the result value of the ith test, n signifies the number of experiments, y_2 denotes the mean, and S_2 is the variance of the experimental data. The purpose of this research is to optimize for maximum TS, FS and IS while minimizing density. The variables examined are BMF content, Nano SiO_2, fiber length, and the concentration of BMF treatment. The components and their respective levels are delineated in Table 2. The orthogonal array used in the experimental design is shown in Table 3. ANOVA confirmed that bamboo fiber content and nano-SiO_2 significantly improved tensile strength, energy absorption, and flexural strength. These nanocomposites are suitable for various industries like automotive and aerospace (Kumar *et al.* 2024).

Table 1. Input parameters and their levels

Factors		Units	Levels			
			1	2	3	4
BMF content	A	%	20	25	30	35
Nano SiO_2	B	%	4	6	8	10
Fiber length	C	mm	6	12	18	24
Sodium hydroxide concentration	D	%	4	8	12	16

Table 2. The factors under consideration in an orthogonal array

Runs	Combination of factors			
	A	B	C	D
1	20	4	6	4
2	20	6	12	8
3	20	8	18	12
4	20	10	24	16
5	25	4	12	12
6	25	6	6	16
7	25	8	24	4
8	25	10	18	8
9	30	4	18	16
10	30	6	24	12
11	30	8	6	8
12	30	10	12	4
13	35	4	24	8
14	35	6	18	4
15	35	8	12	16
16	35	10	6	12

Experiments on the trials (density, TS, FS, and IS tests) were conducted thrice for consistency, and resultant values were subsequently analyzed for optimization and modeling. The effects were optimized

using the Taguchi approach, focusing on maximizing tensile, flexural, and impact properties while minimizing density. A reduction in weight is anticipated to result in less fuel usage and, consequently, a reduction in emissions. Orthogonal experiments using COMSOL Multiphysics showed that fiber contour and size significantly influenced water conductivity and mechanical performance (Bai *et al.* 2024).

The optimal effect is anticipated through the ideal combination, as delineated in Eq (8). Where: T_m represents the total average of density, TS, FS, and IS; k_n signifies the number of primary design elements influencing the output, *and* T_{ijmax} denotes the average effect at the optimal level i of parameter k. T_{ijmax} was derived from the result table of signal to noise ratio or mean, for every variable, the maximum value among the levels represents T_{ijmax}. An ANOVA is performed to evaluate the impact of process variables on the material manufacturing process.

$$T_{\text{opt}} = T_m + \sum_{k=1}^{k_n} [(T_{ik})_{\max} - T_m] \quad \text{... (8)}$$

3.1.2 Confirmation of the Optimization Procedure

The anticipated effects are confirmed by optimally recombining the materials, assessing the different impacts, and comparing the experimental results with the predicted results derived from the CI given by Equation (9).

$$\text{Confidence Interval (C. I)} = \sqrt{F_\alpha(1, F_b) V_b \left[\frac{1}{\eta_{\text{eff}}} + \frac{1}{\eta_{\text{ver}}}\right]} \quad \text{... (9)}$$

Where: F_α (1, F_b) = F ratio mandatory for α; F_b = Error Degrees of Freedom; α = Risk; V_b = Error (derived from ANOVA Table); η_{ver} = number of trials for the confirmation test, equivalent to the quantity of replications for every run; η_{eff} = Effective number of replications, computed utilizing Eq (10), with the percentage error obtained from Eq (11). The percentage error is determined utilizing Eq (11).

$$\eta_{\text{eff}} = \frac{\text{N}}{1+[\text{ Total DOF of controlled parameters }]} \quad \text{... (10)}$$

$$\text{Error} = \frac{\text{observed value - Predictive Value}}{\text{observed Value}} \quad \text{... (11)}$$

3.2 Ranking Methods

3.2.1 CRITIC-ARAS Approach

The CRITIC (CRiteria Importance Through Intercriteria Correlation) approach is used to calculate the objective weights for the chosen criteria by considering their contrast intensity and conflict. This method is employed to commence the ranking process in the first stage. The ARAS method is utilized in the second stage to determine the ranking of the items. Afterwards, the weights obtained from the CRITIC step are used to calculate the composite materials in this research. In particular, an algorithm based on the criteria importance through inter-criteria correlation (CRITIC) and additive ratio assessment (ARAS) methods are used to evaluate several conflicting attributes. A validation through other decision-making techniques was performed to support the robustness of the proposed technique (Lendvai *et al.* 2023).

The optimization process starts with choosing alternatives, identifying attribute, and constructing the decision matrix. The decision matrix is contracted for $\hbar$ alternatives (A_i where i ranges from 1 to $\hbar$) and π attributes (C_j where j ranges from 1 to π).

$$A_i = \begin{vmatrix} c_{11} & c_{12} & \cdots & c_{1j} \\ c_{21} & c_{22} & \cdots & c_{2j} \\ \cdots & \cdots & \cdots & \cdots \\ c_{i1} & c_{i2} & \cdots & c_{ij} \end{vmatrix} \quad \text{... (12)}$$

3.2.2 For Weighting Criteria: CRITIC Approach

The main goal of the initial stage is to determine the comparative advantages of different composite materials in terms of interior, structural design, and aerodynamics applications. The research criteria are depicted at the second level. The material's WA capacity and SHC are additional parameters considered, in addition to its TS, FS, IS and density. The third level of the hierarchy contains the option that is deemed best after materials have been examined. Multi-criteria decision-making (MCDM) using Criteria Importance through Inter criteria Correlation (CRITIC) integrated TOmada de Decisao Interativa Multicriterio (TODIM) methodology was used to find the optimal condition for mechanical properties (Babu *et al.* 2024).

A decision matrix involves the process of normalization. The structured decision-matrix is standardized for the beneficial (N_b) and non – beneficial (N_{nb}) criteria:

$$r_v = \frac{Z_v - \min(Z_v)}{\max(Z_v) - \min(Z_v)}, \text{if} j \in N_b \quad \text{... (13)}$$

$$r_i = \frac{\max(Z_v) - Z_v}{\max(Z_v) - \min(Z_v)} \text{Cif } j \in N_{nb} \quad \text{... (14)}$$

The degree of dispersion for each criterion is measured by determining the standard deviation (Sj) using the following equation:

$$S_j = \sqrt{\frac{\sum_{i=1}^{p} (r_i - \bar{r}_j)^2}{p-1}} \quad \text{... (15)}$$
$$\bar{r}_j = \frac{\sum_{j-1}^{p} r_d}{p}$$

Calculate the correlation coefficient (v_u) for a pair of criteria using Equation (16).

$$v_u = \frac{\sum_{i=1}^{m} (\bar{r}_{ij} - \nabla_j)(\bar{r}_{ik} - \nabla_k)}{\sqrt{\sum_{i=1}^{m} (\bar{r}_{ij} - \nabla_j)^2 \sum_{i=1}^{m} (\bar{r}_{ik} - \nabla_k)^2}} \quad \ldots (16)$$

The symbol ∇_k denotes the average of the k[th] criterion, which is obtained by substituting 'k' with 'j' in Equation 15.

The conflict degree between criteria can be calculated using the calculation provided.

$$M_j = \sum_{i=1}^{q} (1 - v_u) \quad \ldots (17)$$

The coefficient of correlation between the i[th] and j[th] criteria is denoted by v_u.

The formula for calculating the weight (w_j) of the j[th] criterion is as follows:

$$\omega_j = \frac{M_j \times S_j}{\sum_{j-1}^{q} M_j \times S_j} \quad \ldots (18)$$

This alters the atomic structure of the alloy when combined with molybdenum, giving it an unusually high hardness in the overheated form without a purposeful strengthening heat treatment. Fig. 1 shows the prepared specimen for machining with EDM.

3.2.3 For Alternative Ranking: Additive Ratio Assessment (ARAS)

The multi-criteria optimization was conducted on the physical and mechanical properties of the composites using the additive ratio assessment (ARAS) method. This methodology is among the direct methods for implementation and achieving optimal solutions for resolving conflicting multiple-response issues. This approach is frequently utilized to tackle intricate decision-making problems that need the simultaneous evaluation of several factors. Taguchi's design of tests was unable to ascertain the optimal welding parameters that fulfill all welding features. Tensile, flexural, and impact strength are considered advantageous criteria for assessing their maximum values. The density is considered a non-beneficial criterion for establishing its minimum value. The ARAS MCDM method was employed to rank the patterns, highlighting the growing interest in natural fibers for sustainable structural applications (Jha *et al.* 2024).

Step 1: Formation of Decision Matrix

The decision matrix has been created based on the Taguchi design of experimentation. Beneficiary criteria are employed to optimize tensile, flexural, and impact strength. The minimizing density is seen as a 'non-beneficial criterion.

Step 2: Normalized value for beneficial and non-beneficiary criteria

The normalized matrix for the non-beneficiary and beneficiary criterion has been computed using equation (19).

$$N_{ij(b\ \text{benificiary})} = \frac{(\mathrm{T_{ij}})}{\sum_{i=1}^{k} \mathrm{T_{ij}}} \text{ and}$$

$$\check{T}_{ij} = \frac{1}{\mathrm{T_{i(\ (nonbenificiary)}}}, \mathrm{N_{ij\ (non\ benificiary)}} = \frac{(\mathrm{T_{ij}})}{\sum_{i=1}^{k} \mathrm{Y_{ij}}} \quad \ldots (19)$$

The normalized values of beneficiary criteria: tensile, flexural and impact strengths were calculated. The normalized values of non-beneficiary criteria: density is also calculated. The results are displayed in Table 7.

Step 3: Determination of weighted normalized matrix

The weights for the benefit criterion are 0.224, 0.254, and 0.269 for enhancing tensile, flexural, and impact strength, respectively. The weight assigned to minimizing density is 0.253. The equation (20) presents the formula for computing a weighted normalized matrix.

$$\mathrm{WN_{ij}} = \mathrm{W_j} \times \mathrm{N_{ij}} \quad \ldots (20)$$

Where, $\mathrm{W_j}$ weightage to the jth criterion.

The weighted normalized values of each criterion are illustrated in table 8.

Step 4: Determination of optimality function for each alternative solution

The optimality function for each alternative solution has been calculated using equation (21).

$$\mathrm{OF_i} = \sum_{j=1}^{1} \mathrm{WN_{ij}}, \mathrm{i} = 1,2 \ldots, \mathrm{k} \quad \ldots (21)$$

The optimal value for all alternative solutions is ascertained by equation (22).

$$\mathrm{OF_o} = \max \mathrm{OF_i} \quad \ldots (22)$$

Step 6: Determination of utility degree

The utility degree has been computed utilizing OFi and OFo data (equation (23)). The OFi, OFo, and utility degrees are computed and presented in Table 8.

$$\mathrm{UF_i} = \frac{\mathrm{OF_i}}{\mathrm{OF_o}} \quad \ldots (23)$$

Step 7: Ranking of utility degree

The utility degree ranking is conducted to evaluate the optimal and suboptimal alternative options. Experimentation number 7 is chosen to achieve the minimal density while optimizing the flexural, tensile,

and impact strength of the work material, as indicated in table 8. Consequently, 25 BMF content, 8 Nano SiO_2, 4 NaOH concentration and 24 fiber length have been chosen to achieve a density of 0.878 g/cm^3, a flexural strength of 70.1 MPa, a tensile strength of 79.9 MPa and an impact strength of 38.5 kJ/m^2.

3.2.4 Machine Learning (Genetic Algorithm)

Genetic algorithms and other machine learning technologies will be employed to optimize the impacts under investigation. This research employed the GA technique. Objective functions were constructed based on regression models analysing the impact of the Taguchi run combinations. The evolutionary algorithm optimization was conducted using the MATLAB 2023b interface. This study utilizes the default variables of the MATLAB GA optimization. For a population of 20, a scaling function for rank fitness was used to implement a direction of onward migration. In addition to a restricted dependent mutation function and distributed crossover, a crossover probability of 0.8 was used. The stochastic technique was utilized in the models for density, TS, FS and IS. The model derived from the ARAS of the utility degree was refined according to the distinctiveness of the optimization technique.

4. RESULTS AND DISCUSSIONS

Table 3 presents the outcomes of density, flexural, tensile, and impact tests, revealing average strengths of 0.773 g/cm^3, 62.62 MPa, 65.77 MPa, and 26.84 kJ/m^2. The mean signal-to-noise ratios for the TS, FS and IS are 35.89, 36.58, and 27.60, adhering to the principle of "the larger, the better." Conversely, the overall mean for density, following the guideline of "the lower, the better," is 2.305. The response means for the mean and signal-to-noise ratio are shown in Table 4. The Madar fibre content significantly influenced the FS and TS of the composite material, with deltas of 6.97 and 18.42. The BF demonstrated a greater impact on the IS and density of material compared to MF content, achieving the highest ranking. The influence of these elements on the density, flexural, tensile, and impact properties of the material is displayed in Figs. 3–6.

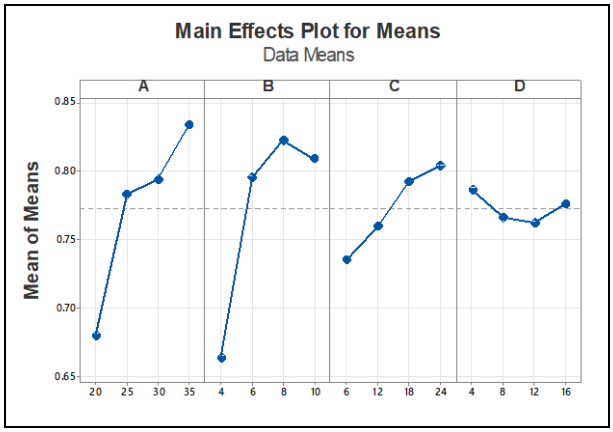

Fig. 3: Main Effects Plot for Density .

Table 3. Experimental results for hybrid composites

S. No.	Output response				S/N Ratios			
	Density	FS	TS	IS	Density	FS	TS	IS
1	0.557	49.1	44.9	5.1	5.083	33.82	33.04	14.15
2	0.684	56.6	54.6	17.6	3.299	35.06	34.74	24.91
3	0.740	64.9	59.1	23.3	2.615	36.24	35.43	27.35
4	0.738	63.4	56.9	21.4	2.639	36.04	35.10	26.61
5	0.638	53.9	62.6	8	3.904	34.63	35.93	18.06
6	0.773	61.6	69.6	24.8	2.236	35.79	36.85	27.89
7	0.878	70.1	79.9	38.5	1.130	36.91	38.05	31.71
8	0.843	65.3	77.1	33.6	1.483	36.30	37.74	30.53
9	0.709	56.7	67.3	26.3	2.987	35.07	36.56	28.40
10	0.848	66	71.2	35.2	1.432	36.39	37.05	30.93
11	0.787	66.5	71.3	29.5	2.081	36.46	37.06	29.40
12	0.832	65.9	71.6	35.3	1.598	36.38	37.10	30.96
13	0.751	58.1	61.6	24.8	2.487	35.28	35.79	27.89
14	0.877	67.5	68	37.5	1.140	36.59	36.65	31.48
15	0.884	70.2	69.6	38	1.071	36.93	36.85	31.60
16	0.823	66.1	67	30.5	1.692	36.40	36.52	29.69
Average	0.773	62.62	65.77	26.84	2.305	35.89	36.28	27.60

Fig. 3 illustrate the impact of several parameters on the density of the fabricated composite. This illustrates the extent to which these variables affect the fuel efficiency of airplanes constructed with composites. It is noted that augmenting BMF content additionally elevates the material's density. These indicate that BMF will adversely affect the fuel consumption of automobiles. It was noticed that augmenting the length of fiber material additionally elevates its density. Nano SiO_2 causes a slight increase in the overall density of the

composite. Significantly, the density of the material was found to decrease as the sodium hydroxide content was increased. This pertains to the extraction of lignin based on the density

Table 4. Table of responses for means

Level	S/N Ratios				Means			
	A	B	C	D	A	B	C	D
Density								
1	3.409	3.615	2.773	2.238	0.6798	0.6637	0.7350	0.7860
2	2.188	2.027	2.468	2.338	0.7830	0.7955	0.7595	0.7662
3	2.024	1.724	2.056	2.411	0.7940	0.8222	0.7922	0.7622
4	1.598	1.853	1.922	2.233	0.8337	0.8090	0.8037	0.7760
Delta	1.811	1.891	0.851	0.177	0.1540	0.1585	0.0687	0.0238
Rank	2	1	3	4	2	1	3	4
Flexural Strength								
1	35.29	34.70	35.62	35.92	58.50	54.45	60.82	63.15
2	35.91	35.96	35.75	35.77	62.72	62.92	61.65	61.63
3	36.07	36.64	36.05	35.92	63.77	67.92	63.60	62.73
4	36.30	36.28	36.16	35.96	65.47	65.17	64.40	62.97
Delta	1.01	1.93	0.54	0.18	6.97	13.48	3.58	1.52
Rank	2	1	3	4	2	1	3	4
Tensile Strength								
1	34.58	35.33	35.87	36.21	53.88	59.10	63.20	66.10
2	37.14	36.32	36.16	36.33	72.30	65.85	64.60	66.15
3	36.94	36.85	36.60	36.23	70.35	69.97	67.88	64.97
4	36.45	36.62	36.50	36.34	66.55	68.15	67.40	65.85
Delta	2.56	1.52	0.73	0.13	18.42	10.87	4.67	1.18
Rank	1	2	3	4	1	2	3	4
Impact Strength								
1	23.25	22.13	25.28	27.07	16.85	16.05	22.48	29.10
2	27.05	28.80	26.38	28.18	26.23	28.78	24.73	26.38
3	29.92	30.01	29.44	26.51	31.57	32.33	30.18	24.25
4	30.16	29.44	29.28	28.62	32.70	30.20	29.97	27.63
Delta	6.91	7.89	4.16	2.12	15.85	16.28	7.70	4.85
Rank	2	1	3	4	2	1	3	4

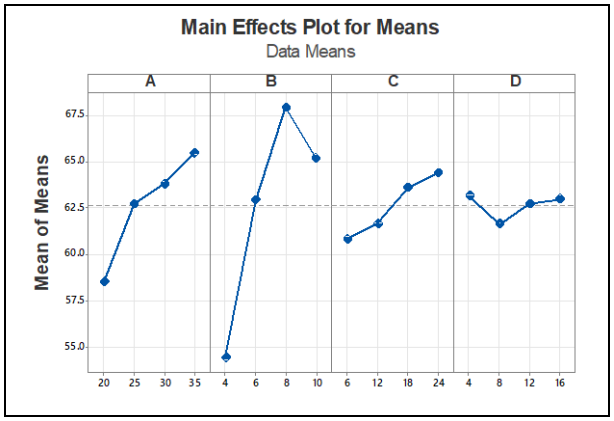

Fig. 4: Main Effects Plot displaying Means of Flexural Strength

Fig. 4 shows that the FS of the NF composite increases with rising BMF content. NFs such as BMF content are recognized for enhancing the FS of polymer composites. The peak FS was recorded at 65.47 MPa with an MF content of 35%.

The maximum FS of 67.92 MPa was achieved with a Nano SiO_2 of 8%, as seen in Fig. 4. The addition of 8% Nano SiO_2 has been found to significantly improve the flexural strength of natural fiber-reinforced composites, such as those incorporating Madar fiber and Bamboo fiber.

Fig. 4 shows the effect of fiber length (C) on the FS of the materials, showing that the rise in FS is essentially linearly proportional to the length of the fibers. This is related to the enhanced transmission of stress from matrix to fibers resulting from the improved surface area. The maximum FS achieved for a fiber length of 24mm was 64.40 MPa.

Fig. 4 illustrates the decrease in flexural strength (FS) when sodium hydroxide (NaOH) concentration increases from 4% to 8%. This reduction may result from inadequate adhesion (lignin elimination) of the fiber surfaces. This results in diminished interfacial adhesion between the matrix and the fibers. The increase in flexural strength over 8% is attributable to the appropriate action of the surface. At elevated concentrations, complete lignin elimination is accomplished, resulting in an enhanced surface roughness conducive to optimal matrix bonding. Four formulations were tested, the bamboo and carbon fibers mixed with polypropylene (8/32/60) hybrid composite showed superior mechanical properties such as flexural strength (76.4 MPa) and impact strength (49.9 kJ/m²), along with enhanced vibrational damping (Kore *et al.* 2021).

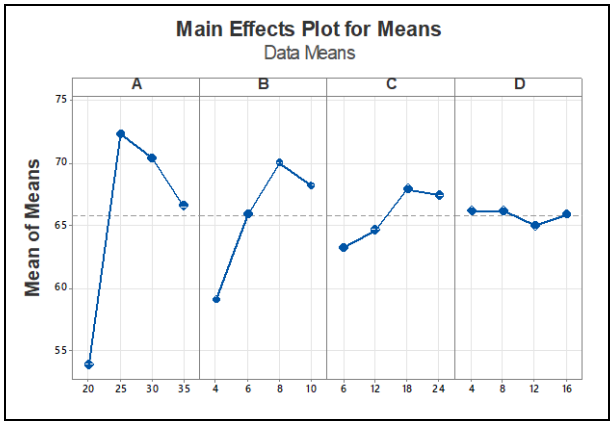

Fig. 5: Main Effects Plot displaying Means of Tensile Strength

Varying fiber lengths and sodium hydroxide (NaOH) concentrations significantly affected the performance of the materials. Longer fibers enhanced tensile, flexural, and impact strengths due to increased surface area for stress transfer, with the optimal length of

24 mm yielding the best results. However, excessively long fibers introduced voids, reducing performance. Similarly, moderate NaOH concentrations (4–8%) improved fiber-matrix bonding by removing lignin and impurities, increasing interfacial adhesion and mechanical properties. Higher NaOH concentrations (>8%) caused fiber damage, reducing tensile strength and impact resistance.

Fig. 5 illustrates that the tensile strength (TS) attains a maximum at a BMF content of 25%, after which a decrease is noted. The principal rise in TS with elevated fiber content is ascribed to the improved interfacial adhesion between fiber and polymer due to NaOH treatment. This may come from the covalent bond between the fiber surface and polymer. The subsequent decline may be ascribed to the rise in fiber ends, resulting in a rise in potential failure initiating locations. Fig. 5 illustrates the addition of 8% Nano SiO_2 offers the best results for enhancing the tensile strength of natural fiber-reinforced composites. Fig. 3 illustrates the enhancement in TS due to the elongation of fiber length. The improvement in TS is due to a larger surface area, which allows for more efficient transmission of stress from the matrix to the reinforcement. Sodium hydroxide exhibits a non-linear impact on the TS of the materials. Although a rise in sodium hydroxide concentration beyond 8% correlates with enhanced tensile strength of the material, the scientists also noted that tensile strength improves with higher alkali treatment concentrations. The variation in TS may be ascribed to the complex interaction between the concentration of NaOH and its influence on the matrix-fiber relationship. Though a small amount of sodium hydroxide concentration does enhance adhesion between the epoxy matrix and fibers, too much treatment can cause over-processing, which in turn causes fiber loss and a decrease in mechanical properties. The reduction in TS at elevated sodium hydroxide concentrations may signify that the harsh treatment has caused fiber breakdown, resulting in diminished load-bearing capacity.

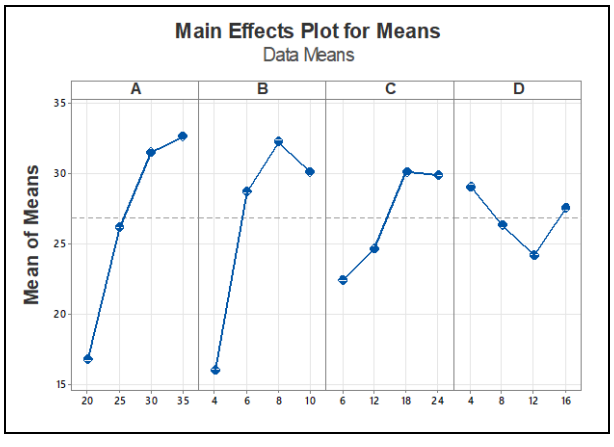

Fig. 6: Main effects plot displaying means of impact strength

Table 5. ANOVA for means in terms of TS, FS, IS, and density

Source	DF	Seq SS	Contribution	Adj MS	F-Value	P-Value
Density						
A	3	0.051706	39.60%	0.017235	47.93	0.005
B	3	0.064651	49.52%	0.021550	59.93	0.004
C	3	0.011767	9.01%	0.003922	10.91	0.040
D	3	0.001354	1.04%	0.000451	1.26	0.428
Error	3	0.001079	0.83%	0.000360		
Total	15	0.130558	100.00%			
R^2 = 99.17%, Adj.R^2 = 95.87%, Pred. R^2 = 76.50%						
Tensile Strength						
A	3	822.87	70.26%	274.289	62.69	0.003
B	3	271.37	23.17%	90.456	20.67	0.017
C	3	60.25	5.14%	20.082	4.59	0.121
D	3	3.57	0.30%	1.189	0.27	0.844
Error	3	13.13	1.12%	4.376		
Total	15	1171.17	100.00%			
R^2 = 98.88%, Adj.R^2 = 94.40%, Pred. R^2 = 68.12%						
Flexural Strength						
A	3	105.882	19.21%	35.294	257.07	0.000
B	3	406.052	73.67%	135.351	985.86	0.000
C	3	33.167	6.02%	11.056	80.53	0.002
D	3	5.632	1.02%	1.877	13.67	0.030
Error	3	0.412	0.07%	0.137		
Total	15	551.144	100.00%			
R^2 = 99.93%, Adj.R^2 = 99.63%, Pred. R^2 = 97.87%						
Impact Strength						
A	3	627.75	40.62%	209.25	14.59	0.027
B	3	646.17	41.81%	215.39	15.02	0.026
C	3	177.91	11.51%	59.30	4.13	0.137
D	3	50.59	3.27%	16.86	1.18	0.449
Error	3	43.03	2.78%	14.34		
Total	15	1545.46	100.00%			
R^2 = 97.22%, Adj.R^2 = 86.08%, Pred. R^2 = 20.80%						

Fig. 6 shows that the maximum IS of the composite with 35% BMF content (A) is 32.70 kJ/m². Although the IS improved with a rise in BMF content, the rate of enhancement reduced beyond 27%. This may result from the creation of voids at elevated content s, which increases potential locations for fracture propagation and initiation. In Fig. 6, an increase in Nano SiO_2 (B) correlates with an enhancement in the material's impact strength. The maximum IS is 32.33 kJ/m² at a Nano SiO_2 composition of 8%. Nano SiO_2 acts as a filler that increases the energy absorption capacity of the composite, enabling it to withstand higher impact forces without failure. Fig. 6 shows that there is a positive correlation between the IS of the composite and the fiber length of the reinforcement fibers. This remains associated with the extensive surface areas that facilitate the efficient transfer of impact energy to the reinforcement. Fig. 6 illustrates the influence of sodium hydroxide (D) on the IS of the synthesized composite. It indicates that under a 4% sodium hydroxide

concentration for fiber treatment, impact strength diminishes as NaOH concentration increases. Exceeding 4%, NaOH positively affects the material's impact strength. The optimal IS achieved for this variable is 29.10 kJ/m².

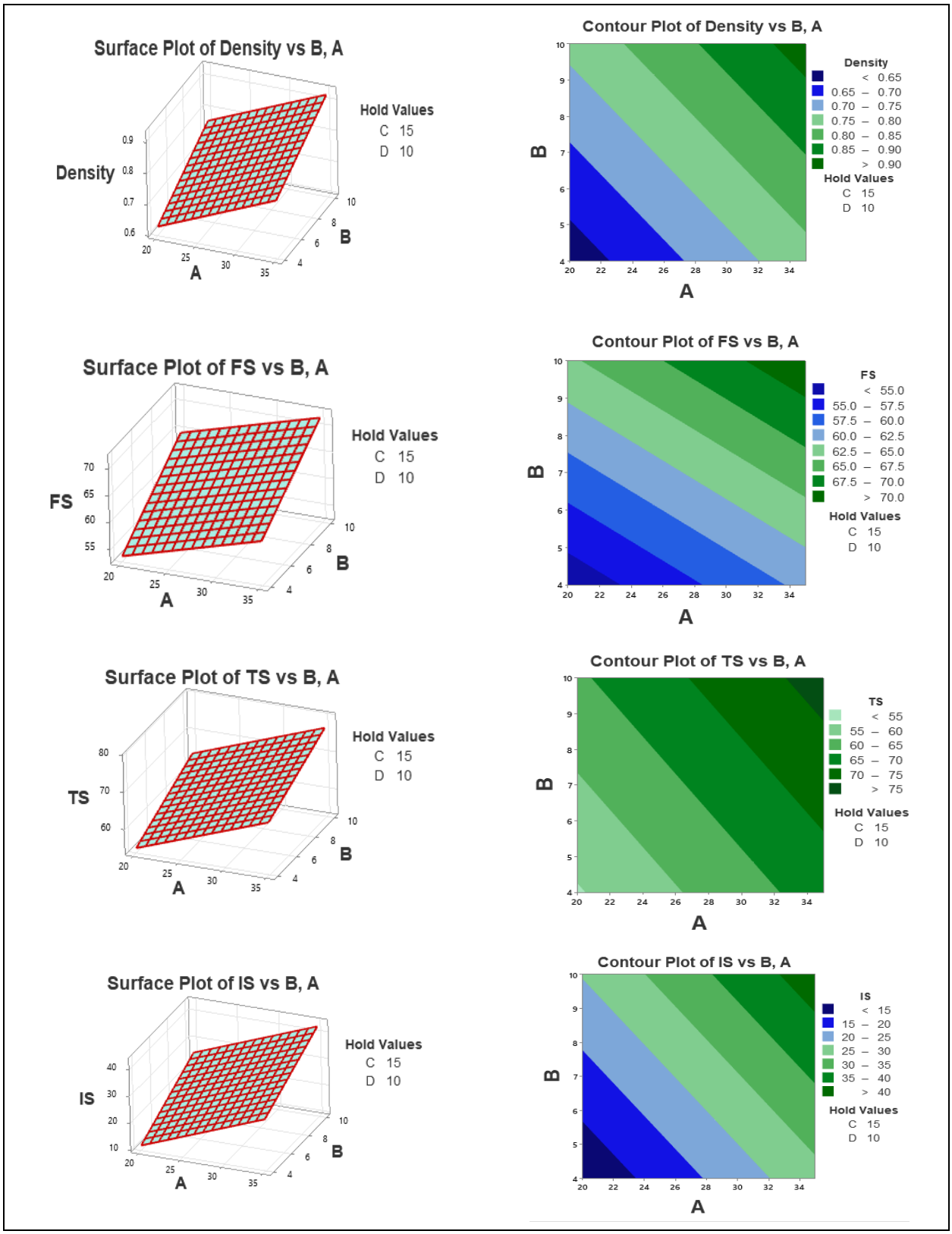

Fig. 7: 2D and 3D plot for MF content and BF content on (a) density, (b) flexural strength, (c) tensile strength and (d) impact strength

4.1 ANOVA for Optimization with a Single Objective

Table 5 displays the variance analysis of several factors on the measured effects, conducted at a 95% confidence level. The incorporation of madar and bamboo fiber significantly influenced the material's tensile strength, with P-values of 0.003 and 0.017, both below 0.05. The BMF content contributed 70.26% to the TS of the material. All parameters under examination significantly influence the FS of the composite designed for airplane body applications, with P-values < 0.05. Nano SiO_2 contributed 73.67% to the material's FS, whereas BMF content accounted for 19.21%. The intrinsic stability of the material was markedly influenced by the bamboo fiber and Nano SiO_2, exhibiting P-values of 0.026 and 0.027, with contributions (%) of 41.81% and 40.62%. The IS of the matrix is improved by this fiber reinforcement, which has a minimum IS. The amount of surface area that can bond to the matrix is also determined by the fiber length. The content of BMF, Nano SiO_2, and fiber length significantly affected the material's density. The carbon emissions of an airplane will be significantly affected by a decrease of BMF, Nano SiO_2, and length of fiber in the composite materials utilized in automobile development. It is essential to recognize that the manufacture of BMF generates greater emissions of carbon and contributes more to global warming than the manufacturing of natural fibers.

Figs. 7(a–d) illustrates interaction graphs depicting the influence of BMF content and Nano SiO_2 on TS, FS, impact energy, and density. Fig. 7a demonstrates that fluctuations in BMF and Nano SiO_2 substantially influence the material's density. Materials used for airplane structures must be lightweight; hence, a reduced number of denser materials, such as BMF, is required, while a greater quantity of natural fibers. Fig. 7b demonstrates that the interaction between BMF content and Nano SiO_2 significantly affected the FS at 20–35% and 4–10%. Fig. 7c demonstrated a considerable interaction between BMF content and Nano SiO_2 on the TS of the materials. The tensile strength was found to be optimal with BMF content between 20–35% and Nano SiO_2 between 4–10%. Furthermore, Fig. 7d demonstrates that the interplay among fiber content produces notable variations in the material's IS. The maximum IS was achieved with BMF content above 35%. The use of NFs is advantageous for the environment, as they are biodegradable, and their incorporation into automobile constructions is consistent with sustainable practices.

4.2 Optimization with a Single Objective

Table 6 shows the appropriate configurations of the process variables to achieve superior performance. The composite containing 20% BMF, 4% Nano SiO_2, a length of 6mm fiber, and a sodium hydroxide concentration of 12% exhibited the lowest density. The proposed material for automobile body application exhibits a proven TS of 79.9 MPa, achieved with a 35% BMF content, an 8% Nano SiO_2, a length of fiber 6 mm, and a sodium hydroxide concentration of 4% for fiber treatment. A BMF content of 25%, a Nano SiO_2 of 8% with a length of fiber 24 mm, and a sodium hydroxide treatment concentration of 4% yielded the optimal FS of 70.2 MPa. Furthermore, the optimal combination of process parameters, including BMF content 25%, Nano SiO_2 8%, a length of fiber 18mm, and a sodium hydroxide concentration of 4%, yielded the highest IS of 38.5 kJ/m².

Table 6. The best solutions to get the different effects

Serial no	Effects	Best Solution				Units	Pred. Opt. result	Confirmed Opt. result
		A (%)	B (%)	C (mm)	D (%)			
1.	Density	20	4	6	12	g/cm^3	0.523	0.577
2.	FS	35	8	24	4	MPa	78.99	79.9
3.	TS	25	8	18	4	MPa	73.09	70.2
4.	IS	35	8	18	4	kJ/m^2	43.79	38.5

Materials engineered for automobile applications are anticipated to possess high toughness and IS to endure conditions, for example, bird strikes or impacts at transport. The density of the resultant substance was markedly decreased at the ideal combination. Reducing the density of material used in airplanes immediately reduces carbon emissions and operating costs. Consequently, the automobile sector, in addition to structural integrity, has championed the use of lightweight materials. The incorporation of reinforcement, especially in treated NF materials, can decrease material weight; nevertheless, a possible disadvantage is the emergence of pores, which may result from the random distribution of fibers within the matrix or from the manufacturing procedure. The creation of pores in the composite may compromise its structural integrity by serving as localized sites for crack initiation; depending on their morphology, these voids can also function as limited areas for crack mitigation. Figs. 8a and b present the scanning electron microscope images of the combination from run 1 (the minimum performance) alongside the optimal combination identified using ARAS. The pores seen in the designed composite classify them as fracture mitigators rather than imperfections. The analysis indicated that the poorest performers had a greater number of pores, as illustrated in Fig. 8 a, while the highest performers displayed less pores, as shown in Fig. 8b. The superior composite probably exhibited enhanced interfacial adhesion among the epoxy and fibers matrix. Improved adhesion inhibits void formation and delamination under load, leading to a reduction in voids and a more uniform fractured surface. Various fracture-toughening mechanisms such as fiber debonding and crack deflection were observed, providing

insights for optimizing bamboo structures and fiber-reinforced composites (Wang *et al.* 2023).

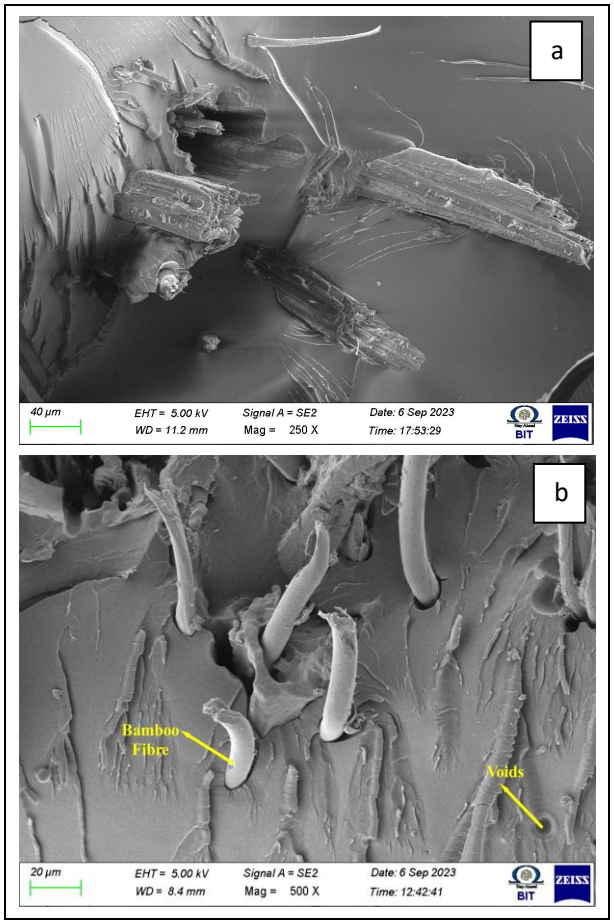

Fig. 8: Scanning electron microscope picture on (a) composite material with the lowest performance, (b) optimal composite material with the highest performance

4.3 Regression Analysis for Optimization with a Single Objective

Regression modeling was used to assess the material's density, FS, TS and IS properties. The developed models were utilized to predict the various characteristics of the composites across multiple conceivable combinations of the process variables. The models are delineated in Eq (24–27). Additionally, exceptional R-Square values were achieved, indicating the models' great reliability in forecasting the mechanical properties of the materials. The accuracy metrics of the models for FS, TS, and IS are notable, with R-Squared values of 82.22%, 89.26%, and 85.13%. The density model, which correlates straight with the carbon emissions of automobiles, had a maximum forecast accuracy of 89.31%.

Density = 0.240 + 0.00933 BMF + 0.0105 NS + 0.0034 fiber length + 0.0178 NaOH concentration + 0.000118 BMF*NaOH concentration + 0.00152 NS* fiber length - 0.00099 B*NaOH concentration - 0.000993 fiber length *NaOH concentration … (24)

FS = 31.4 + 0.462 BMF + 0.94 NS + 0.271 fiber length + 0.94 NaOH concentration + 0.0021 BMF* NaOH concentration + 0.074 NS* fiber length - 0.018 NS* NaOH concentration - 0.0572 fiber length * NaOH concentration … (25)

TS = 9.4 + 0.595 BMF + 3.02 NS - 0.214 fiber length + 3.99 NaOH concentration + 0.0252 BMF* NaOH concentration + 0.215 NS* fiber length - 0.463 NS* NaOH concentration - 0.0993 fiber length * NaOH concentration … (26)

IS = -27.4 + 0.766 BMF + 2.46 NS + 0.21 fiber length + 1.24 NaOH concentration + 0.0394 BMF* NaOH concentration + 0.138 NS* fiber length - 0.214 NS* NaOH concentration - 0.0657 fiber length * NaOH concentration … (27)

4.4 ARAS

ARAS is a statistical method employed to identify the optimal point at which emissions of carbon, relative to material weight, are minimized while structural reliability (TS, FS, and IS) is maximized. It was utilized to determine the optimal solution of production factors for the materials that minimize carbon emissions while maximizing structural durability. Table 7 shows the succession of departures from unity (1) and the normalizing of the means for measured effect. Additionally, it presents the calculated OF_i, utility degree, and corresponding rankings for each. Run 7, possessing the maximum rank, exhibits a process variable combination of 30% BMF content, 8% Nano SiO_2, 18mm length of fiber, and 4% sodium hydroxide. The overall mean was calculated to be 0.777. Table 9 displays the response table for the utility degree (UFi). BMF significantly affects the mechanical properties of materials used in automobile structure development. The BMF, ranked 2 with a delta of 0.1402, has the second most substantial impact on the mechanical behaviours of materials in aeronautical design. Fig. 9 illustrates the influence of several production variables on the ARAS, indicating its possible applicability as an automobile material. Fig. 9 shows that BMF loading enhances the ARAS within the optimal range of 9% to 30%. BMF positively influences the development of automobiles, facilitating reduced emissions while ensuring structural reliability. The influence diminishes beyond this point, resulting in minimal change. This indicates that BMF can successfully substitute the volume proportion of Nano SiO_2 in the construction of automobile structural materials while maintaining substantial structural integrity. The observed favorable influence reduces with Nano SiO_2 beyond 8%, potentially due to the creation of detrimental microstructures, such as voids, inside the material.

Table 7. Decision matrix and normalized matrix for the ARAS method

S. No.	Decision matrix				1/D	Normalized matrix			
	TS	FS	IS	Density		TS	FS	IS	Density
Optimum Value	**79.9**	**70.2**	**38.5**	**0.557**	**1.794**	0.0706	0.0655	0.0823	0.0786
1	44.9	49.1	5.1	0.557	1.794	0.0397	0.0458	0.0109	0.0786
2	54.6	56.6	17.6	0.684	1.461	0.0482	0.0528	0.0376	0.0640
3	59.1	64.9	23.3	0.740	1.352	0.0522	0.0605	0.0498	0.0592
4	56.9	63.4	21.4	0.738	1.355	0.0503	0.0591	0.0457	0.0594
5	62.6	53.9	8	0.638	1.568	0.0553	0.0503	0.0171	0.0687
6	69.6	61.6	24.8	0.773	1.293	0.0615	0.0575	0.0530	0.0567
7	79.9	70.1	38.5	0.878	1.139	0.0706	0.0654	0.0823	0.0499
8	77.1	65.3	33.6	0.843	1.186	0.0681	0.0609	0.0718	0.0519
9	67.3	56.7	26.3	0.709	1.411	0.0594	0.0529	0.0562	0.0618
10	71.2	66	35.2	0.848	1.179	0.0629	0.0616	0.0752	0.0516
11	71.3	66.5	29.5	0.787	1.270	0.0630	0.0620	0.0630	0.0557
12	71.6	65.9	35.3	0.832	1.202	0.0632	0.0615	0.0754	0.0527
13	61.6	58.1	24.8	0.751	1.332	0.0544	0.0542	0.0530	0.0584
14	68	67.5	37.5	0.877	1.140	0.0601	0.0630	0.0801	0.0500
15	69.6	70.2	38	0.884	1.132	0.0615	0.0655	0.0812	0.0496
16	67	66.1	30.5	0.823	1.215	0.0592	0.0617	0.0652	0.0532
Weight	0.224	0.254	0.269	0.253					

Table 8. Obtaining an optimum solution using the ARAS method

S. No.	Weighted Normalization				OFi	UFi	Rank
	TS	FS	IS	Density			
Optimum Value	0.0158	0.0167	0.0221	0.0199	0.0745	1.000	
1	0.0089	0.0116	0.0029	0.0199	0.0433	0.582	16
2	0.0108	0.0134	0.0101	0.0162	0.0505	0.679	14
3	0.0117	0.0154	0.0134	0.0150	0.0555	0.745	11
4	0.0112	0.0150	0.0123	0.0150	0.0536	0.720	13
5	0.0124	0.0128	0.0046	0.0174	0.0471	0.633	15
6	0.0137	0.0146	0.0143	0.0143	0.0570	0.765	10
7	0.0158	0.0166	0.0221	0.0126	0.0672	0.902	1
8	0.0152	0.0155	0.0193	0.0132	0.0632	0.848	5
9	0.0133	0.0135	0.0151	0.0156	0.0575	0.772	9
10	0.0141	0.0157	0.0202	0.0131	0.0630	0.846	6
11	0.0141	0.0158	0.0170	0.0141	0.0609	0.818	7
12	0.0141	0.0156	0.0203	0.0133	0.0634	0.851	4
13	0.0122	0.0138	0.0143	0.0148	0.0550	0.738	12
14	0.0134	0.0160	0.0216	0.0126	0.0636	0.855	3
15	0.0137	0.0167	0.0218	0.0126	0.0648	0.870	2
16	0.0132	0.0157	0.0175	0.0135	0.0599	0.805	8

Table 9. Mean and signal to noise ratio response table for utility degree

Level	S/N Ratios				Means			
	A	B	C	D	A	B	C	D
1	-3.369	-3.390	-2.664	-2.090	0.6815	0.6812	0.7425	0.7975
2	-2.157	-2.126	-2.486	-2.295	0.7870	0.7863	0.7583	0.7708
3	-1.712	-1.602	-1.899	-2.466	0.8217	0.8337	0.8050	0.7573
4	-1.773	-1.893	-1.960	-2.159	0.8170	0.8060	0.8015	0.7817
Delta	1.657	1.788	0.765	0.376	0.1402	0.1525	0.0625	0.0402
Rank	2	1	3	4	2	1	3	4

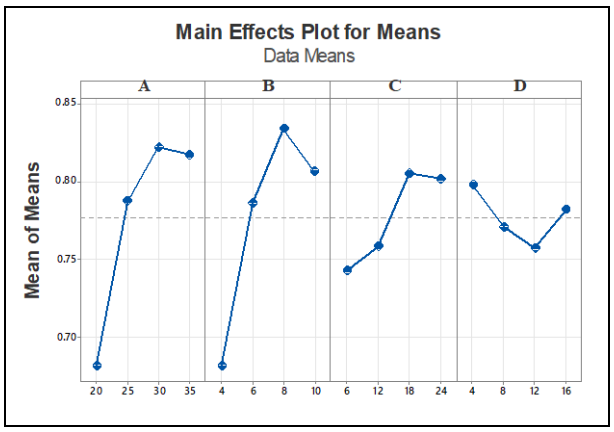

Fig. 9: Main effects plot displaying means of ARAS

Typically, enhancing the length of fiber enhances the performance of the NF hybrid material in aeronautical applications, as illustrated in Fig. 9. It diminishes the carbon emissions of automobiles. The energy required for producing short-fiber materials surpasses that of longer-fiber composites, attributable to the greater number of steps involved. The optimum utility degree (UFi) was seen at the 18 mm length of the fiber. The linear relationship indicates that a fiber length above 18% will enhance the material's performance.

Fig. 9 indicates that within the NaOH concentration range of 4 – 8%, the material's efficacy for structural growth diminishes. Even though the fiber surface may become smooth when lignin is removed, there may still be insufficient interfacial adhesion between the matrix and fiber material. However, beyond a sodium hydroxide concentration of 4%, the material's performance improves. This results in optimum interfacial adhesion and a rough texture due to the proper alkalization of the fiber surfaces.

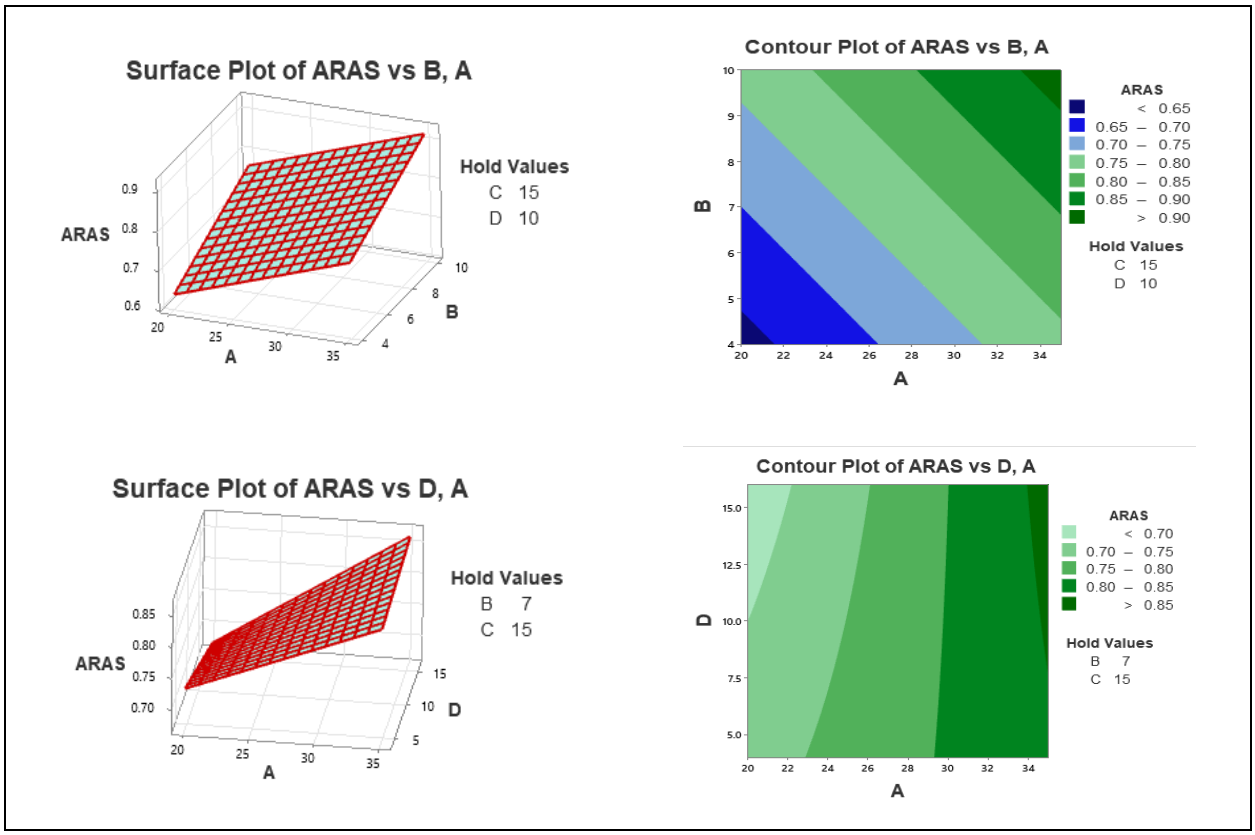

Fig. 10: 3D and 2D plots on utility degree (UFi) in (a) MF loading and BF loading (b) MF loading and NaOH concentration

4.5 ANOVA for the Utility Degree

Table 10 displays the ANOVA for the means of utility degree (UFi). With a 95% degree of confidence (P-value less than 0.05), it was determined that the length of fiber exerted the greatest substantial effect on the utility degree, with a P-value of 0.048, which is below 0.05. The performance of polymer composite materials used in airplane construction is greatly influenced by the length of the fibers used in their manufacture. It can significantly influence the automobile's carbon emissions. The performance of the utility degree was influenced by the fiber length at 8.23%. Fig. 10a (i) (ii) graphically illustrates the relationship among MF content and BF content on the utility degree using 3D and 2D contour plots. The optimal utility degree (greatest

material performance regarding airplane application) occurred with MF content between 20% and 35% and BF content between 5% and 15%. Furthermore, Fig. 10b (i) (ii) illustrates the correlation between MF content and sodium hydroxide concentration during treatment. The optimal ARAS performance occurred with BMF content between 20% and 35%.

Table 10. ANOVA on the utility degree means

Source	DF	Seq SS	Contribution	Adj MS	F-Value	P-Value
Regression	8	0.106422	86.93%	0.013303	5.82	0.016
A	1	0.038940	31.81%	0.002085	0.91	0.371
B	1	0.035575	29.06%	0.002432	1.06	0.337
C	1	0.010013	8.18%	0.000009	0.00	0.048
D	1	0.000738	0.60%	0.001696	0.74	0.418
A*D	1	0.001474	1.20%	0.001474	0.64	0.448
B*C	1	0.000597	0.49%	0.003214	1.41	0.275
B*D	1	0.013850	11.31%	0.008707	3.81	0.092
C*D	1	0.005235	4.28%	0.005235	2.29	0.174
Error	7	0.016006	13.07%	0.002287		
Total	15	0.122428	100.00%			

4.6 The Utility Degree Optimization and Validation

The utility degree was tuned for a greater value, indicating superiority. The utility degree response tables indicated that optimal performance occurred with a process variable mix of 30% BMF content, 8% Nano SiO_2, a fiber length of 18mm, and a concentration of 4% NaOH. The calculated ARAS averages at these levels were 0.8217, 0.8337, 0.8050, and 0.7975. The optimal utility degree, as predicted by Eq (8), is 0.817. The validation of forecast was achieved by fabricating the composite materials using the optimal parameter combination.

4.7 Modeling and Regression Analysis for the Utility Degree

The utility degree was analyzed by regression modeling. The derived model is articulated in Eq (21). The R^2 value of 86.93% and the adjusted R^2 value of 71.98% show a commendable dependability in the model that forecasts the suitability of composites for automobiles, depending on the analyzed variables: BMF content (A), Nano SiO_2 (B), fiber length (C), and concentration of sodium hydroxide (D).

ARAS = 0.299 + 0.00613 BMF + 0.0227 NS - 0.0007 fiber length + 0.0152 NaOH concentration + 0.000419 BMF* NaOH concentration + 0.00167 NS* fiber length - 0.00259 NS* NaOH concentration - 0.000673 fiber length * NaOH concentration … (28)

4.8 Genetic Algorithm

The fitness function for the GA was derived using the models derived from the Taguchi orthogonal array regression study. The optimal function of fitness for the optimization of the single-objective of the ARAS method is illustrated in Fig. 11.

It usually happens that the fitness of one generation gets passed down to the next. The optimal values for density, tensile strength, flexural strength, and IS were determined to be 0.4421 g/cm³, 60 MPa, 63.11 MPa, and 92.21 kJ/m². The optimal values for the fitness function of the utility degree were found to be 1. The GA approach demonstrates a reduced computation time for optimizing parameter fitness. Based on a GA applied to the ARAS function, the best solution for optimizing the performance of generated composite for airplane constructions is 35% BMF, 10% Nano SiO_2, 24mm of fiber length, and 9% sodium hydroxide concentration.

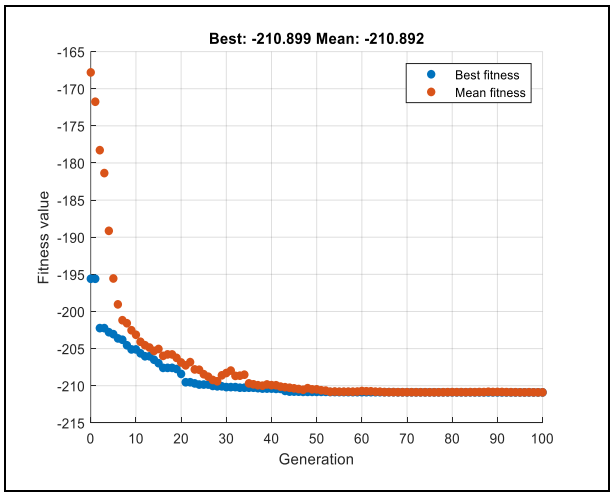

Fig. 11: ARAS best fitness

5. CONCLUSION

The GA approach of ML was utilized to optimize the process variables for producing NF-reinforced polymer materials for automobile applications in structural, aiming to diminish emissions of carbon resulting from fuel consumption. As a lightweight material for environmentally friendly, minimum-emission, a composite made of MF and BF can be produced.

The optimal density, TS, FS and IS of the produced composites, utilizing Taguchi single objective optimization approach, are 0.577 g/cm³, 79.9 MPa, 73.09 MPa, 38.5 kg/m². The MF content, BF content, length of fiber, and sodium hydroxide concentration significantly influence the TS, FS, and IS of the material, as

demonstrated by ANOVA. Additionally, it is observed that their weight has a major effect on the automobile's carbon emissions. Regression models for density, TS, FS, and IS exhibited prediction accuracies of 99.17%, 98.88%, 99.93%, and 97.22%. ARAS-based multi-objective optimization revealed that a process variable combination of 30% bMF content, 8% Nano SiO_2, 18mm length of fiber, and 4% sodium hydroxide concentration is the best choice for creating materials for airplane structures with low carbon emissions.

At a 95% confidence level, the variance analysis of the utility degree shows that the MF content significantly affects the development of automobile materials with the goal of lowering carbon emissions (P-value < 0.05). The GA analysis of the models showed that 35% BMF, 10% Nano SiO_2, 24mm fiber length, and 9% sodium hydroxide concentration are the best process factors for making hybrid composite with least emissions of carbon airplane structures.

This research establishes a foundation for mitigating greenhouse gas emissions in the automobile sector through material innovation. The examination of comprehensive sustainability (the creation of entirely natural materials without synthetic components) was not conducted, leaving a need for future research.

FUNDING

This research received no specific grant from any funding agency in the public, commercial, or not-for-profit sectors.

CONFLICTS OF INTEREST

The authors declare that there is no conflict of interest.

COPYRIGHT

REFERENCES

Abessolo, D., Biwole, A. B., Fokwa, D., Ganou Koungang, B. M. and Baah, Y. B., Physical, Mechanical and Hygroscopic Behaviour of Compressed Earth Blocks Stabilized with Cement and Reinforced with Bamboo Fibres, *Int. J. of Engg. Res. in Africa*, 59, 29–41 (2022). https://doi.org/10.4028/p-spbskv

Babu, K. A., Paramasivam, B., Vijayananth, K., Seenivasan, V. and Raju, S., Effect of eggshell powder on polyvinyl ester composite: A statistical correlation on mechanical strength, *Environ. Prog. Sustain Energy*, 43(4), (2024). https://doi.org/10.1002/ep.14382

Bai, Y., Yang, W., Shi, B., Liu, L., Wang, M., Wang, S., Song, X. and Tian, C., Optimization Design and Analysis of Irregular Cross-Sectional Structure in Water Conducting Fibers, *Geotech. Geol. Eng.*, 42(7), 6147–6164 (2024). https://doi.org/10.1007/s10706-024-02897-z

Bajaro, M. L. G. and Silva, D. L., Hybrid Particle Swarm Optimization — Artificial Neural Network: Strength Prediction of Bambusa Blumeana Fiber and Recycled Coarse Aggregate for Multi-generation Recycled Aggregate Concrete, In: 2023 *IEEE 3rd International Conference on Software Engineering and Artificial Intelligence)*, *IEEE*, 75–79 (2023). https://doi.org/10.1109/SEAI59139.2023.10217632

Chandrika, V. S., Anamika, A., Jeeva, C., Perumal, B., Kumar, S. S., Roseline, J. F. and Raghavan, I. K., Natural Fiber Incorporated Polymer Matrix Composites for Electronic Circuit Board Applications, *Adv. Mater. Sci. Eng.*, 2022, 1–9 (2022). https://doi.org/10.1155/2022/3035169

Cui, J., Fu, D., Mi, L., Li, L., Liu, Y., Wang, C., He, C., Zhang, H., Chen, Y., and Wang, Q., Effects of Thermal Treatment on the Mechanical Properties of Bamboo Fiber Bundles, *Mater.*, 16(3), 1239 (2023). https://doi.org/10.3390/ma16031239

Elango, M., Naveen, K. V., Annamalai, A. and Harish, P., Prediction of Tensile Strength of Hybrid Natural Fiber Reinforced Composites Using Machine Learning Approach, *Adv. Mech. Mater. Technol.*, 491–501 (2022). https://doi.org/10.1007/978-981-16-2794-1_44

Ganta, M. G. and Patel, M., Experimental Comparison of the Effect of Fiber Orientation on Mechanical Properties of Natural Fiber Reinforced Composites (NFRCs), *J. Inst. Eng. India Ser. D*, 105(2), 975–981 (2024). https://doi.org/10.1007/s40033-023-00520-8

Gorrepotu, S. R., Debnath, K. and Mahapatra, R. N., Multi-response Optimization of the Chemical Treatment Process Parameters Influencing the Tensile, Flexural, Compression, and Shear Properties of the Injection Moulded Green Composites, *J. Polym. Environ.*, 31(1), 112–130 (2023). https://doi.org/10.1007/s10924-022-02613-z

Jha, M. K., Gupta, S., Chaudhary, V. and Gupta, P., Selection and prioritization of weaving structure of reinforced fiber for better performance, *AIP Conf. Proc.*, 2835(1), 020018 (2024), https://doi.org/10.1063/5.0221447

Anand, K. J. and Ekbote, T., Experimental Investigations on Physical and Mechanical Properties of Hybrid Bamboo Composites, *Frattura ed Integrità Strutturale*, 18(69), 29–42 (2024). https://doi.org/10.3221/IGF-ESIS.69.03

Kavimani, V., Paramasivam, B., Sasikumar, R. and Venkatesh, S., A CRITIC integrated WASPAS approach for selection of natural and synthetic fibers embedded hybrid polymer composite configuration, *Multiscale Multidiscip. Model. Exp. Des.*, 7(3), 1721–1736 (2024). https://doi.org/10.1007/s41939-023-00301-6

Kore, S., Spencer, R., Ghossein, H., Slaven, L., Knight, D., Unser, J. and Vaidya, U., Performance of hybridized bamboo-carbon fiber reinforced polypropylene composites processed using wet laid technique, *Composites Part C*, 6, 100185 (2021). https://doi.org/10.1016/j.jcomc.2021.100185

Kumar, R., Ganguly, A. and Purohit, R., Optimization of mechanical properties of bamboo fiber reinforced epoxy hybrid nano composites by response surface methodology, *Int. J. Interact. Design and Manufacturing*, 18(9), 6479–6492 (2024). https://doi.org/10.1007/s12008-023-01215-w

Lendvai, L., Singh, T., Rigotti, D. and Pegoretti, A., Thermally conductive and electrically resistive acrylonitrile butadiene styrene (ABS)/boron nitride composites: Optimal design using a multi-criteria decision-making approach, *J. Mater. Res. Technol.*, 26 8776–8788 (2023). https://doi.org/10.1016/j.jmrt.2023.09.165

Marichelvam, M. K., Kumar, C. L., Kandakodeeswaran, K., Thangagiri, B., Saxena, K. K., Kishore, K., Wagri, N. K. and Kumar, S., Investigation on mechanical properties of novel natural fiber-epoxy resin hybrid composites for engineering structural applications, *Case Stud. Constr. Mater.*, 19(13), e02356 (2023). https://doi.org/10.1080/15440478.2021.1875368

Natrayan, L., Ashok, S. K., Kaliappan, S. and Kumar, P., Effect of Stacking Sequence on Mechanical Properties of Bamboo/Bagasse Composite Fiber for Automobile Seat Cushions and Upholstery Application, 2024(1), 5013(2024), https://doi.org/10.4271/2024-01-5013

Premnath, K., Arunprasath, K., Sanjeevi, R., Elilvanan, R. and Ramesh, M., Natural/synthetic fiber reinforced hybrid composites on their mechanical behaviors– a review, *Interactions*, 245(1), 111 (2024). https://doi.org/10.1007/s10751-024-01924-y

Quan, W., Huang, W., An, Y,. Miao, X. and Chen, Z., The effect of natural bamboo fiber and basalt fiber on the properties of autoclaved aerated concrete, *Constr. Build Mater.*, 377 131153 (2023). https://doi.org/10.1016/j.conbuildmat.2023.131153

Raja, T., Devarajan, Y. and Thanappan, S., Studies on the mechanical and thermal stability of Calotropis gigantea fibre-reinforced bran nano particulates epoxy composite, *Sci. Rep.*, 13(1), 16291 (2023). https://doi.org/10.1038/s41598-023-42316-6

Raja, T., Mohanavel, V., Kannan, S., Parikh, S., Paul, D., Velmurugan, P., Chinnathambi, A., Alharbi, S. A. and Sivakumar, S., The effect of porcelain filler particulates madar fiber reinforced epoxy composite – A comprehensive study for biomedical applications, *Heliyon*, 10(8), e29818 (2024a). https://doi.org/10.1016/j.heliyon.2024.e29818

Raja, T., Yuvarajan, D., Ali, S., Dhanraj, G. and Kaliappan, N., Fabrication of glass/madar fibers reinforced hybrid epoxy composite: a comprehensive study on the material stability, *Sci. Rep.*, 14(1), 8374 (2024b). https://doi.org/10.1038/s41598-024-53178-x

Richmond, T., Lods, L., Dandurand, J., Dantras, E., Lacabanne, C., Malburet, S., Graillot, A., Durand, J. M., Sherwood, E. and Ponteins, P., Physical and dynamic mechanical properties of continuous bamboo reinforcement/bio-based epoxy composites, *Mater. Res. Express*, 9(1), 015505 (2022). https://doi.org/10.1088/2053-1591/ac4c1a

Saha, A., Kulkarni, N. D. and Kumari, P., Development of Bambusa tulda-reinforced different biopolymer matrix green composites and MCDM-based sustainable material selection for automobile applications, *Environ. Dev. Sustain.*, (2023). https://doi.org/10.1007/s10668-023-04327-1

Tadesse, M., Sinha, D. K., Gutu, J. M., Jameel, M., Hossain, N., Jha, P., Gupta, G., Zainuddin, S. and Ahmed, G. M. S., Optimization of Tailor-Made Natural- and Synthetic-Fiber-Reinforced Epoxy-Based Composites for Lightweight Structural Applications, *J. Compos. Sci.*, 7(10), 443 (2023). https://doi.org/10.3390/jcs7100443

Vijayan, R., Natarajan, E., Palanikumar, K., Krishnamoorthy, A., Markandan, K. and Ramesh, S., Effect of hybridization and stacking sequences on mechanical properties and thermal stability of aloe vera-roselle-glass fiber reinforced polymer composites, *Polym. Compos.*, 44(10), 6593–6603 (2023). https://doi.org/10.1002/pc.27582

Vijayananth, K., Paramasivam, B. and Raju, S., Measurement of mechanical and thermal performance of cigarette filter fibres/eggshell particles reinforced polymer composite using integrated CRITIC-TODIM approach, *Measurement*, 228, 114251 (2024). https://doi.org/10.1016/j.measurement.2024.114251

Wang, X., Chen, X., Huang, B., Chen, L., Fang, C., Ma, X. and Fei, B., Gradient changes in fiber bundle content and mechanical properties lead to asymmetric bending of bamboo, *Constr Build Mater*, 395 132328 (2023). https://doi.org/10.1016/j.conbuildmat.2023.132328

Yoganandam, K., Ramshankar, P., Ganeshan, P. and Raja, K., Mechanical properties of alkali-treated Madar and Gongura fibre-reinforced polymer composites, *Int. J. Ambient Energy*, 41(8), 849–850 (2020). https://doi.org/10.1080/01430750.2018.1477066

Yusoff, R. B., Takagi, H. and Nakagaito, A. N., A comparative study of polylactic acid (PLA)-Based unidirectional green hybrid composites reinforced with natural fibers such as kenaf, bamboo and coir, *Hybrid Adv.*, 3 100073 (2023). https://doi.org/10.1016/j.hybadv.2023.100073

Zhao, C., Li, T. and Li, W., Mechanical Analysis of Ice-Composite and Fibber Strength by Daily Tools, *J. Phys. Conf. Ser.*, 2083(2), 022014 (2021). https://doi.org/10.1088/1742-6596/2083/2/022014